Variable Signal Progression Bands for Transit Vehicles Under Dwell Time Uncertainty and Traffic Queues

Hyeonmi Kim, Yao Cheng, and Gang-Len Chang, *Member, IEEE*

***Abstract*— Signal priority controls have long been viewed as one of the viable strategies to minimize bus delays at intersections so as to reduce the travel time variability or increase headway stability. Such control strategies, however, are often not effective for arterials serving heavy bus flows, because frequent signal priority calls will inevitably disrupt the arterial signal plan and incur excessive delays to general traffic. To overcome such deficiencies, this paper presents a bus-based signal progression model for arterials with heavy bus flows as in most major cities in Asia and Europe. The proposed model features its properties of accounting for the impacts of average bus dwell time, its variance, and the bus stop capacity. The impacts of various upstream traffic flow rates and signal plans on the available bus progression band have also been included in computing the optimal bus-progression offsets. Extensive simulation experiments have confirmed the effectiveness of the computed bus progression bands under various traffic congestion levels. The proposed bus-based pre-timed signal system can serve as a base plan for real-time operations of priority control for bus progression if the congestion level on the arterial or dwelling time variance as well as traffic queues have exceeded the operational capacity of the bus-based progression system.**

***Index Terms*— Bus progression, stochastic bus dwell times, traffic queues**

I. Introduction

INCREASING transit system ridership has long been recognized as one of the potentially effective strategies to mitigate urban traffic congestion from the demand side. However, a variety of factors associated with transit operations (e.g., uncertain waiting times at bus stops, variable travel times, and frequent stops at traffic signals) often cause transit system unfavorable in comparison with the auto mode. In an attempt to enhance transit service reliability, over the past decades a rich body of research has proposed various Transit Signal Priority (TSP) strategies, which allow a bus to pass an intersection without delays. Those studies can be classified into two classes: passive or active control, and the later one contains unconditional or conditional priority. Passive TSP control is typically operated without detectors, based mainly on the off-line information of transit routes and ridership patterns, and considered effective under high transit vehicle frequencies, predictable transit travel times, and light or moderate traffic volumes [1]. In contrast, active TSP control demands the placement of bus detectors at the target intersection to exercise a green extension or red truncation based on the detected bus information. Despite the effectiveness of the unconditional active TSP on improving bus efficiency, some concerns have also been raised about its potential negative impacts on the side street traffic and the signal coordination if frequently requested or when excessive activations occur for buses ahead of schedule [2]–[3].

In response to such challenges, many researchers have proposed conditional active TSP, which sets constraints on granting signal priority, including the maximum number of priority calls over a preset period, consistent cycle lengths, and only for buses behind the schedule [4]–[9]. However, the effectiveness of these strategies diminishes, when the bus volume increases, because some percentage of buses behind schedule will not experience the signal priority and the negative impacts on side street and general traffic may also negate the total benefits for such control. In addition, despite a rich body of research on adaptive network traffic control [10]–[13] or urban traffic control [14]–[17] over the past decades, only a few cities have actually deployed such signal control systems in a small network due to the concerns of operating costs and required expertise. These real-time strategies may be further constrained by their demands of data quality and the long-lasting maintenance issues. Hence, a passive control strategy, considering the bus flow patterns in design of off-line signal control, emerges as one viable cost-benefit option. Such a control can offer the potential for use on arterials without on-line surveillance and also serve as the basis for minimizing TSP activation in various real-time control systems.

In developing signal control strategies for off-line operations in networks, the main design notion has long been either to maximize the progression or to minimize the total delay. On the subject of maximizing the progression band, Morgan and Little [18] presented a pioneering model to maximize the two-way progression bandwidth, and Little [19] later advanced the model to concurrently optimize the cycle length, progression speeds, and offsets with integer programming. Little *et al.* [20] further enhanced the model for application, named MAXBAND, by accounting for left-turn treatments and the impacts of initial queues.

Manuscript received September 12, 2016; revised June 23, 2017 and December 18, 2017; accepted January 24, 2018. The Associate Editor for this paper was I. Papamichail. *(Corresponding author: Yao Cheng.)*

The authors are with the Department of Civil and Environmental Engineering, University of Maryland, College Park, MD 20742 USA (e-mail: hmkim@umd.edu; ycheng09@umd.edu; gang@umd.edu).

Color versions of one or more of the figures in this paper are available online at http://ieeexplore.ieee.org.

Digital Object Identifier 10.1109/TITS.2018.2801567

Grounded on the same logic, Gartner *et al.* [21], Chaudhary *et al.* [22] and Yang *et al.* [23] proposed various formulations to reflect the needs of different bandwidths for links or paths with different volumes. Papola [24] proposed a model that can produce split solutions and concluded that the differences between solutions of split and unsplit types are negligible for an arterial with a large number of signals. Messer *et al.* [25] extended the progression model to allow the selection among different phase sequence plans. Tsay and Lin [26] and Lin *et al.* [27] considered queuing vehicles on a major-street approach to discharge and leave the intersection. Li [28] took into account the progression time uncertainty in design of a two-phase control method to produce an optimal plan under varying progression time. Some researchers, including Yang *et al.* [29], Chang *et al.* [30], Chaudhary and Messer [31], and Gartner and Stamatiadis [32] and [33], also extended Little's arterial progression models to various applications, ranging from an unconventional intersection to grid networks. Along the same line, Zhang *et al.* [34] developed an Asymmetrical Multi-BAND (AM-BAND) model to better utilize the available green times by allowing the bands to be asymmetrical with respect to the progression line. However, these progression models are designed mainly for passenger cars, and thus do not often benefit those bus flows which need to stop at stations. Hence, under the objectives of improving bus service quality, providing reliable travel time, and enticing more commuters to choose the bus mode, implementing the bus-based signal progression is one of the potentially effective strategies.

On this regard of improving the operational efficiency of transit systems with traffic signal designs, only a limited number of studies are reported in the literature. For example, Ma and Yang [35] developed a passive signal priority approach for Bus Rapid Transit system by analyzing the traffic signal status upon bus arrival to an intersection. Lin *et al.* [36] proposed a passive control strategy for urban arterials by adding a constant dwell time on computation of bus travel time between two intersections. Dai *et al.* [37] analyzed the relation between bus green band and general vehicle green band and developed a model to minimize bus dwell time, based on predetermined maximum and minimum bus bands and general vehicle bands. Their method accounted for benefits to both bus and general vehicles, but needs adjustments to the bus dwell time or travel time with on-board devices. They considered the potential impact of bus dwell time, but did not model the impact due to the stochastic nature of dwell times. Dai *et al.* [38] further constructed a progression model by categorizing intersections into different groups, based on the location of bus stops and the expected dwell time. To address the impact of the stochastic dwell time, Cheng *et al.* [39] proposed a preliminary model to compute the offset for a bus-based progression for arterials with heavy transit flows using the same logic of MAXBAND. However, traffic queue at the intersection contributed by unsynchronized vehicles and their resulting impacts on design of signal progression offsets has not been considered.

Thus, this paper has presented a bus-based signal progression system to improve the bus service reliability, and also to promote the bus mode for urban commuters under existing signal control environments. The proposed system has offered the following key features which have not been addressed adequately in the literature but are critical to the design of a bus-based signal progression system:

(1) Offering a tool for transportation agencies to address the delays or local congestions issues (e.g., intersection long queues caused by bus flows due to their operational characteristics) by converting the classical signal progression to the bus-based signal progression design without any additional investment.

(2) Producing the bus-based progression bands that minimize the impacts of bus operations on the general traffic flows, which can also concurrently improve the quality of bus services, such as reducing the number of signal-incurred stops, improving schedule reliability.

(3) Functioning as an effective passive bus priority system to circumvent the need for deploying individual intersection-based bus detectors for active bus priority control along an arterial.

(4) Accounting for critical factors (i.e., bus dwell time, bus speed, bus stop capacity, and interference with passenger cars), affecting the effectiveness of bus progression, but not yet adequately addressed in the literature in design of bus progression signal control.

(5) Incorporating the impacts of intersection traffic queues, due to passenger car flows, in computing the progression bands for bus flows along an arterial without exclusive bus lanes, a quite complex but critical task to ensure the sufficient width and reliability (i.e., minimizing the impacts by traffic queues) for the resulting progression bands.

(6) Embedding the uncertainties due to dwell time variation in formulating the model for the bus-based signal progression, which can minimize the impacts of the inevitable demand variation at each bus stop on the resulting signal offsets for bus progression, an imperative factor that has not been addressed in the TSP control literature.

In summary, this research has been conducted along the line of passive urban TSP control to facilitate bus operations, but not in the category of network traffic control even through an effective bus progression can certainly minimize the impacts of heavy bus flows on the overall traffic conditions.

II. Modeling Methodology

To successfully progress buses over intersections, the proposed model for computing signal offsets shall take into account the following issues: dwell times and their variance at bus stops, bus stop capacity, and traffic queues at intersections.

A. Modeling Bus Dwell Time Uncertainty at a Bus Stop

As shown in Fig. 1 (a), if a bus dwells at a stop, it is likely to deviate away from the progression band designed for passenger cars and encounter a red phase at the downstream intersection. Hence, to ensure the signal progression for buses, it is necessary to take into account the impacts of bus dwell times on their travel times between intersections. Note that although bus dwell time can be controlled with the information

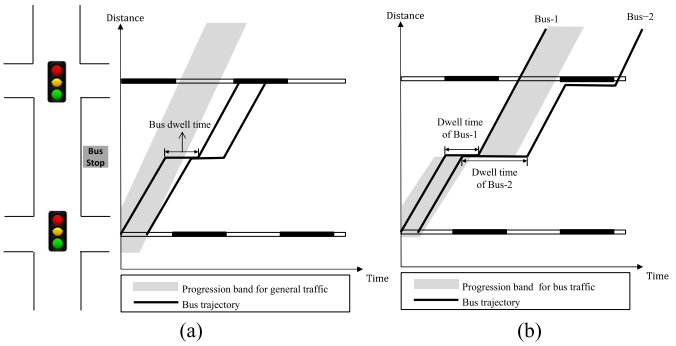

Fig. 1. Bus progression with bus dwell time uncertainty: (a) Impacts of bus dwelling at a bus stop on the progression and (b) Stochastic nature of bus dwell times and its impact on progression.

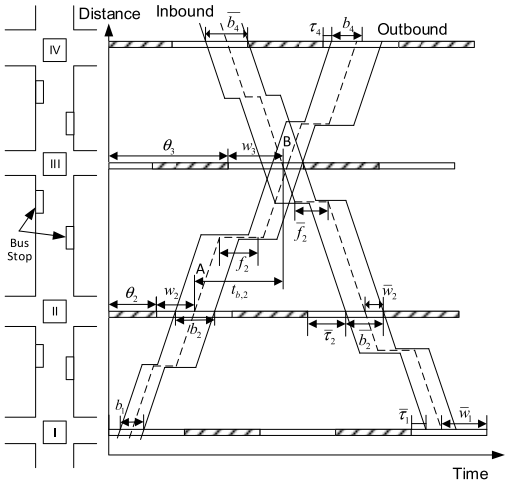

Fig. 2. Variable progression bands.

from bus GPS and on-board units, its stochastic nature correlates highly with transit demands at each stop. Fig. 1 (b) depicts an example of such impacts on the bus progression, where Bus-1 receives a green phase at the downstream intersection but Bus-2 does not since its dwell time is longer. Hence, dwell time variance is one of the critical issues in design of an effective transit signal progression system.

One alternative to address this issue is to introduce a variable-band scheme that allows the bandwidth to vary along an arterial, as shown in Fig. 2. Unlike the typical signal progression for passenger cars which takes each intersection as a control point [21], the proposed bus progression model views each bus stop as a control point. In other words, the change in bandwidths will take place only at a bus stop, and the transition between two consecutive bands (i.e., bands that are arriving at and departing from a bus stop) may determine the effectiveness of the entire system's performance.

Although several plans may yield the identical total bandwidth, the resulting performance for bus flows can be quite different. For example, a wider arriving band in Fig. 3 (a) can certainly receive more buses, but only a few of those can be expected to stay in the departing band toward the downstream intersection due to the inevitable dwell time variation. In contrast, a narrower arriving band as shown in Fig. 3 (b)

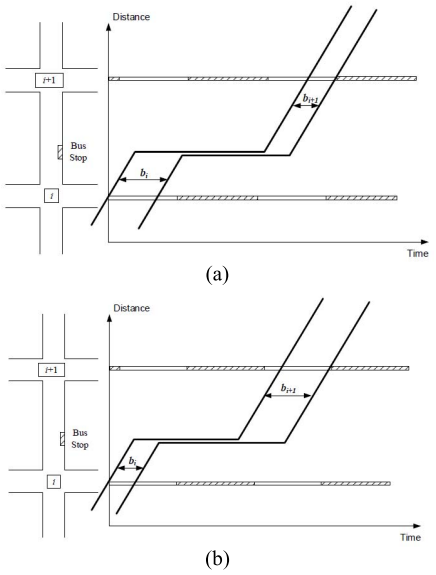

Fig. 3. Relationship between neighboring bands at a bus stop. (a) A wide arriving band with a narrow departing band; and (b) A narrow arriving band with a wide departing band.

may receive fewer buses from the upstream, but most of such can leave the stop within the departing band. Although these two plans yield the identical total bandwidth, the resulting bus delays are quite different. Thus, the effectiveness of a bus progression plan depends on not only the total progression bandwidth but also the relationship between the arriving and departing bands at each bus stop. To estimate whether or not a bus can pass through consecutive intersections without encountering a red phase, one should estimate the likelihood (the statistical expectation of the probability) that a bus can stay in the departing band after leaving the bus stop.

B. Capacity of Bus Stops

Another critical issue to be addressed in design of a bus progression system is the storage capacity of bus stops. If more buses are arriving at a bus stop than its storage capacity, the queuing buses may spill back to the nearby intersection and block traffic flows to the intersection. Such spillovers can result in the following issues: 1) causing potential safety concerns at the upstream intersection near the bus stop, 2) increasing the delay of vehicles approaching the intersection, 3) increasing the total delays for buses arriving at the bus stop, and 4) contributing to the bus dwell time uncertainty. Hence, in design of a bus-based progression, one shall preset an upper bound for the bus bandwidth so that the number of buses arriving at a bus stop in a short period will be less likely to exceed the available storage.

C. Impacts of Intersection Traffic Queue

In a bus progression system, passenger cars not within a bus band may encounter a red phase at traffic signals, and thus form the initial queue during the red phase. Hence, to ensure the progression for buses, offsets between signals shall be

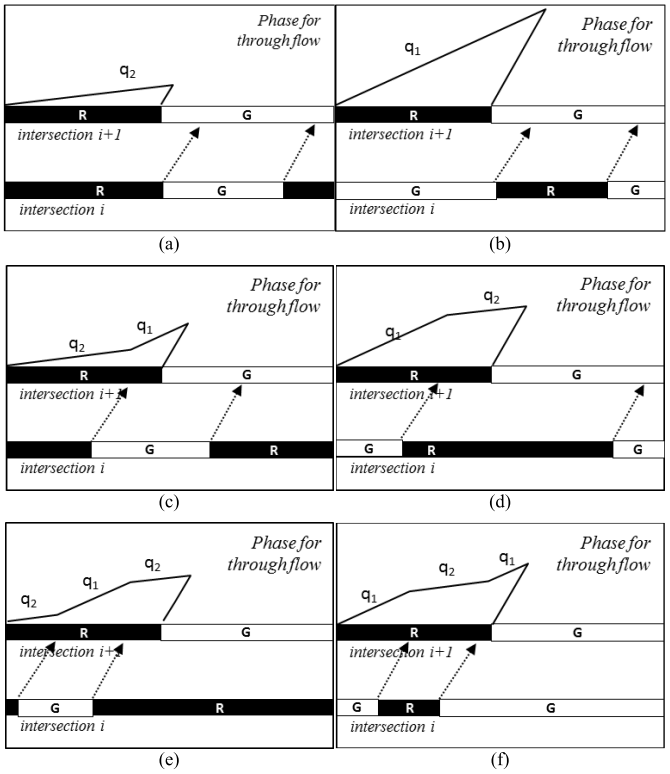

Fig. 4. Six vehicle arrival pattern types and resulting intersection queue formation and discharging. (a) Type 1: All through vehicles from the upstream intersection encounter a green phase at the downstream intersection. (b) Type 2: Through vehicles from the upstream intersection encounter the green-red-green phases at the downstream intersection. (c) Type 3: Through vehicles from the upstream intersection encounter the red-green phases at the downstream intersection. (d) Type 4: Through vehicles from the upstream intersection encounter the green-red phases at the downstream intersection. (e) Type 5: All through vehicles from the upstream intersection encounter a red phase at the downstream intersection. (f) Type 6: Through vehicles from the upstream intersection encounter the red-green-red phases at the downstream intersection.

designed to accommodate clearance times for such a queue. Note that traffic queues at an intersection are contributed to by incoming flows from two sources, through and turning vehicles at the upstream intersection. Arrival flow patterns to the target intersection are the results of complex interactions between traffic conditions, distance between neighboring intersections, and signal plan such as offsets and green intervals. Traffic queues actually vary with arriving flow patterns during a red phase, and the resulting clearance time is a function of the queue length and the arrival rate during the discharging period.

Assuming that traffic volumes and travel times between intersections are constant during a cycle, one can then estimate the initial queue length and clearance time for a set of offsets between two intersections. Given the traffic volumes, passenger car travel times between intersections, and signal timings, one can categorize vehicle arrival patterns into the following six types for estimating queue accumulation and discharging, as shown in Fig. 4. For example, there will be a short traffic queue if turning vehicles from an upstream intersection (q_2) arrive at the target intersection during queue forming and discharging (Fig. 4 (a)). On the other hand, traffic queue will be long if higher through flows from an upstream

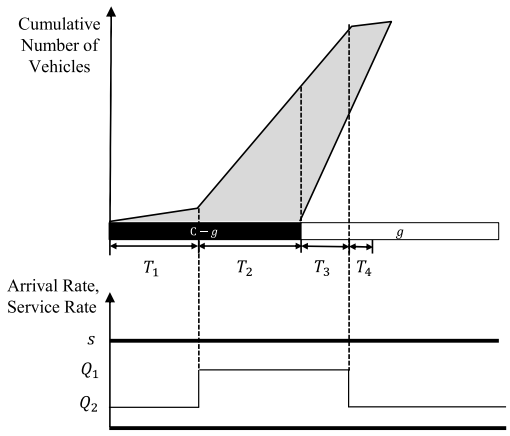

Fig. 5. Time intervals during queue formation and discharging.

intersection (q_1) arrive at the target intersection during queue forming and discharging (Fig. 4 (b)).

Furthermore, for Type 1 to Type 4, arrival rate during queue discharging at the target intersection can have a transition between two incoming flow sources based on offsets of pairwise intersections and green interval of an upstream intersection (see transition between T_3 and T_4 in Fig. 5). Hence, in design of a bus-based progression, one should consider the impacts of intersection traffic queue due to passenger-car flows and estimate the queue clearance time based on offsets and upstream traffic flows.

III. Model Formulations

This section presents two sets of formulations for the bus progression design, where the first is a direct extension of MAXBAND but accounts for the average bus dwell time at a bus stop, capacity of a bus stop, and traffic queues at signals. The second takes into account the stochastic nature of bus dwell times with variable bandwidths along an arterial. Key notations used in these two proposed models are shown in Table 1.

A. Model 1: A Base Model for Bus Progression

As discussed previously, with the identified information such as phase plans, traffic flow patterns, bus headways, and bus dwell time, one can directly extend MAXBAND with the following objective function for offset optimization:

$$Max\ b + k_b \bar{b} \tag{1}$$

$$(1 - k_b)\,\bar{b} \geq (1 - k_b)\,k_b b \tag{2}$$

where k_b is a weighting factor of the bandwidth for the inbound direction, and should be determined by the ratio between inbound and outbound bus volume. Eq. (2) will ensure that the bandwidth for the less favored direction would remain within a reasonable range. The key to ensure the progression for buses, however, depends on the specification of the following constraints.

1) Interference Constraints: The first group, named the directional interference constraints, is to ensure that the bus progression bands use only the available green time subtracted

TABLE I
KEY NOTATIONS

Notation	Description
	Parameters
N	Total number of intersections
$g_i\ (\bar{g}_i)$	The outbound(inbound) green interval at intersection i (sec)
r_i	Time difference between the start of the outbound green and the end of the inbound green at intersection i (sec)
$t_{c,i}\ (\bar{t}_{c,i})$	Average outbound (inbound) travel time for passenger cars from intersection i (i+1) to intersection i+1 (i) (sec)
$t_{b,i}\ (\bar{t}_{b,i})$	Average outbound (inbound) travel time for buses from intersection i (i+1) to intersection i+1 (i), which is sum of bus running time and bus dwell time (sec)
$d_i\ (\bar{d}_i)$	Distance from intersection i (i+1) to intersection i+1 (i) (ft)
$v_{b,i}\ (\bar{v}_{b,i})$	Average bus running speed from intersection i (i+1) to intersection i+1 (i) (ft/sec)
$f_i\ (\bar{f}_i)$	Average dwell time at the outbound(inbound) bus stop after (before) intersection i (i+1) (sec)
$\sigma_i(\bar{\sigma}_i)$	Standard deviation of dwell times for the outbound (inbound) buses at the stop ahead of intersection i (i+1)
$m_i\ (\bar{m}_i)$	The expected number of outbound (inbound) buses passing intersection i during the synchronized phase in one hour
$\phi_i\ (\bar{\phi}_i)$	Weighting factor for the outbound (inbound) bandwidth at intersection i
C	Cycle length (sec)
k_b	Directional weighting factor
s	Saturation flow rates (veh/hr)
$q_{1,i}\ (\bar{q}_{1,i})$	Average discharging rate of thru movement of intersection i (i+1) to intersection i+1(i) (veh/hr)
$q_{2,i}\ (\bar{q}_{2,i})$	Average discharging rate of turning movement of intersection i (i+1) to intersection i+1(i) (veh/hr)
$L_i\ (\bar{L}_i)$	Number of lanes for outbound (inbound) through movement at intersection i
$b_i^{\max}\ (\bar{b}_i^{\max})$	Upper bound of bus outbound (inbound) bandwidth at intersection I (sec)
M	A large positive number
	Variables
$b\ (\bar{b})$	Bus outbound (inbound) bandwidth (sec)
$b_i\ (\bar{b}_i)$	Bus outbound (inbound) bandwidth at intersection i (sec)
$b_i^e\ (\bar{b}_i^e)$	Effective outbound (inbound) bandwidth at intersection i for buses (sec)
$w_i\ (\bar{w}_i)$	Time period between the start (end) of a green phase and the center of the bus band at intersection i for the outbound (inbound) direction (sec)
θ_i	Offset at intersection i
$T_{1,i}\ (\bar{T}_{1,i})$	Time interval used for queue to accumulate before there is a change in arrival flows at intersection i (sec)
$T_{2,i}\ (\bar{T}_{2,i})$	Time interval used for queue to accumulate after there is a change in arrival flows at intersection i (sec)
$T_{3,i}\ (\bar{T}_{3,i})$	Time interval used for queue to discharge before there is a change in arrival flows at intersection i (sec)
$T_{4,i}\ (\bar{T}_{4,i})$	Time interval used for queue to discharge after there is a change in arrival flows at intersection i (sec)
$\gamma_{1,i}\ (\bar{\gamma}_{1,i})$	Time difference between onset of green and arrival of first possible thru leading vehicle from the upstream intersection at intersection i (sec)
$\gamma_{2,i}\ (\bar{\gamma}_{2,i})$	Time difference between onset of green and arrival of first possible turning leading vehicle from the upstream intersection at intersection i (sec)
$\tau_i\ (\bar{\tau}_i)$	Queue clearance time for outbound (inbound) at the intersection i (sec)
$x_{1,i}\ (\bar{x}_{1,i})$	Binary variable indicating the phase that the first vehicle of outbound (inbound) traffic flows from the main streets at the intersection i encountered
$x_{2,i}\ (\bar{x}_{2,i})$	Binary variable indicating the phase that the last vehicle of outbound (inbound) traffic flows from the main streets outbound (inbound) at the intersection i encountered
$x_{3,i}\ (\bar{x}_{3,i})$	Binary variable indicating if there is a change in the phases that outbound (inbound) through or turning vehicles from upstream intersection i-1 (i+1)
$s_i\ (\bar{s}_i)$	Binary variable ensuring the upper bound of bus bandwidth
$n_i\ (\bar{n}_i)$	Integer variable to represent the number of signal cycles for progression constrains
$c_{1,i}\ (\bar{c}_{1,i})$ $c_{2,i}\ (\bar{c}_{2,i})$	Integer variable to represent the number of signal cycles for traffic queue constrains

by the initial queue clearance time at intersection i. Such constraints can be specified as follows:

$$w_i - 0.5b \geq \tau_i \quad \text{for } i = 1, \ldots, N \tag{3}$$

$$w_i + 0.5b \leq g_i \quad \text{for } i = 1, \ldots, N \tag{4}$$

$$w_i - 0.5\bar{b} \geq 0 \quad \text{for } i = 1, \ldots, N \tag{5}$$

$$\bar{w}_i + 0.5\bar{b} \leq \bar{g}_i - \bar{\tau}_i \quad \text{for } i = 1, \ldots, N \tag{6}$$

As shown in Fig. 2, Eqs. (3) and (6) indicate that the start of green bands should not be within the queue clearance time, while Eqs. (4)-(5) force the bands to end within a green phase.

2) Progression Constraints: The second group is a set of progression constraints specified to ensure that the center line of the progression bands passes through the green phases under the specified offsets. Each constraint functions to limit the difference between the centers of the inbound or outbound bands for each pair of neighboring intersections to be equal to the travel time on that link. For a pair of neighboring intersections, i and $i+1$, one can express the progression constraints as follows:

$$\begin{aligned} &\theta_i + w_i + t_{b,i} + C \times n_i \\ &= \theta_{i+1} + w_{i+1} + C \times n_{i+1} \quad \text{for } i = 1, \ldots, N-1 \end{aligned} \tag{7}$$

$$\begin{aligned} &-\theta_i - r_i + \bar{w}_i + \bar{t}_{b,i} + C \times \bar{n}_i \\ &= -\theta_{i+1} - r_{i+1} + \bar{w}_{i+1} + C \times \bar{n}_{i+1} \quad \text{for } i = 1, \ldots, N-1 \end{aligned} \tag{8}$$

The bus travel times, $t_{b,i}(\bar{t}_{b,i})$, between intersections i ($i+1$) and $i+1$ (i) specified in the progression constraints are the sum of bus running time and dwell time at a bus stop. These terms are defined in (9) and (10), where, $d_i(\bar{d}_i)$ is the distance between intersection i ($i+1$) to intersection $i+1$ (i); $v_{b,i}(\bar{v}_{b,i})$ indicates the average bus running speed from intersection i ($i+1$) to intersection $i+1$ (i); and $f_i(\bar{f}_i)$ denotes the average dwell time. For those links without a bus stop, the average dwell time is set to be zero.

$$t_{b,i} = \left(\frac{d_i}{v_{b,i}} + f_i\right) \quad \text{for } i = 1, \ldots, N-1 \tag{9}$$

$$\bar{t}_{b,i} = \left(\frac{\bar{d}_i}{\bar{v}_{b,i}} + \bar{f}_i\right) \quad \text{for } i = 1, \ldots, N-1 \tag{10}$$

Taking an example for links between II and III as shown in Fig. 2, the left side of Eq. (7) refers to the horizontal coordinate of Point A plus the travel time, while the right side refers to the distance from Point B to the vertical axis. Forcing these two terms to be equal can make sure that the bands are continuous along the links.

3) Bus Stop Capacity Constraints: The third group is constraints for bus stop capacity to ensure that the number of buses arriving at a bus stop within the bands does not exceed the available storage at a bus stop. This is fulfilled by setting the upper bound on the bus bandwidth based on the bus arrival rate. Assuming that the bus arrival to each stop follows a Poisson distribution, the probability for k buses to be in the outbound green band i can be expressed as follows:

$$f(k) = \frac{(\lambda b_i)^k \times e^{-\lambda b_i}}{k!} \tag{11}$$

TABLE II
TIME INTERVALS FOR QUEUE CLEARANCE TIME

Type	$T_{1,i}(\bar{T}_{1,i})$	$T_{2,i}(\bar{T}_{2,i})$	$T_{3,i}(\bar{T}_{3,i})$	$T_{4,i}(\bar{T}_{4,i})$
1	0	$C-g_i$ $(C-\bar{g}_i)$	$Min\left[\left(q_{2,i-1}\times(C-g_i)\right)/(s\times L_i-q_{2,i-1}),-\gamma_{1,i}\right]$ $\left(Min\left[\left(\bar{q}_{2,i+1}\times(C-g_i)\right)/(s\times\bar{L}_i-\bar{q}_{2,i+1}),-\bar{\gamma}_{1,i}\right]\right)$	$\left(q_{2,i-1}\times(C-g_i)-(q_{2,i-1}-s\times L_i)\times T_{3,i}\right)/(s\times L_i-q_{1,i-1})$ $\left(\left(\bar{q}_{2,i+1}\times(C-\bar{g}_i)-(\bar{q}_{2,i+1}-s\times\bar{L}_i)\times\bar{T}_{3,i}\right)/(s\times\bar{L}_i-\bar{q}_{1,i+1})\right)$
2	0	$C-g_i$ $(C-\bar{g}_i)$	$Min\left[\left(q_{1,i-1}\times(C-g_i)\right)/(s\times L_i-q_{1,i-1}),-\gamma_{2,i}\right]$ $\left(Min\left[\left(\bar{q}_{1,i+1}\times(C-\bar{g}_i)\right)/(s\times\bar{L}_i-\bar{q}_{1,i+1}),-\bar{\gamma}_{2,i}\right]\right)$	$\left(q_{1,i-1}\times(C-g_i)-(q_{1,i-1}-s\times L_i)\times T_{3,i}\right)/(s\times L_i-q_{2,i-1})$ $\left(\left(\bar{q}_{1,i+1}\times(C-\bar{g}_i)-(\bar{q}_{1,i+1}-s\times\bar{L}_i)\times\bar{T}_{3,i}\right)/(s\times\bar{L}_i-\bar{q}_{2,i+1})\right)$
3	$C-g_i-T_{2,i}$ $(C-\bar{g}_i-\bar{T}_{2,i})$	$\gamma_{1,i}$ $(\bar{\gamma}_{1,i})$	$Min\left[g_{i-1}-\gamma_{1,i},\left(q_{2,i-1}\times(C-g_i-\gamma_{1,i})+q_{1,i-1}\times\gamma_{1,i}\right)/(s\times L_i-q_{1,i-1})\right]$ $\left(Min\left[\bar{g}_{i+1}-\bar{\gamma}_{1,i},\left(\bar{q}_{2,i+1}\times(C-\bar{g}_i-\bar{\gamma}_{1,i})+\bar{q}_{1,i+1}\times\bar{\gamma}_{1,i}\right)/(s\times\bar{L}_i-\bar{q}_{1,i+1})\right]\right)$	$\left(q_{2,i-1}\times(C-g_i-\gamma_{1,i})+q_{1,i-1}\times\gamma_{1,i}-(q_{1,i-1}-s\times L_i)\times T_{3,i}\right)/(s\times L_i-q_{2,i-1})$ $\left(\left(\bar{q}_{2,i+1}\times(C-\bar{g}_i-\bar{\gamma}_{1,i})+\bar{q}_{1,i+1}\times\bar{\gamma}_{1,i}-(\bar{q}_{1,i+1}-s\times\bar{L}_i)\times\bar{T}_{3,i}\right)/(s\times\bar{L}_i-\bar{q}_{2,i+1})\right)$
4	$C-g_i-T_{2,i}$ $\left(C-\bar{g}_i-\bar{T}_{2,i}\right)$	$\gamma_{2,i}$ $(\bar{\gamma}_{2,i})$	$Min\left[C-g_{i-1}-\gamma_{2,i},\left(q_{1,i-1}\times(C-g_i-\gamma_{2,i})+q_{2,i-1}\times\gamma_{2,i}\right)/(s\times L_i-q_{2,i-1})\right]$ $\left(Min\left[C-\bar{g}_{i+1}-\bar{\gamma}_{2,i},\left(\bar{q}_{1,i+1}\times(C-g_i-\bar{\gamma}_{2,i})+\bar{q}_{2,i+1}\times\bar{\gamma}_{2,i}\right)/(s\times\bar{L}_i-\bar{q}_{2,i+1})\right]\right)$	$\left(q_{1,i-1}\times(C-g_i-\gamma_{2,i})+q_{2,i-1}\times\gamma_{2,i}-(q_{2,i-1}-s\times L_i)\times T_{3,i}\right)/(s\times L_i-q_{1,i-1})$ $\left(\left(\bar{q}_{1,i+1}\times(C-\bar{g}_i-\bar{\gamma}_{2,i})+\bar{q}_{2,i+1}\times\bar{\gamma}_{2,i}-(\bar{q}_{2,i+1}-s\times\bar{L}_i)\times\bar{T}_{3,i}\right)/(s\times\bar{L}_i-\bar{q}_{1,i+1})\right)$
5	g_{i-1} $(\bar{g}_{i+1})$	$C-g_i-g_{i-1}$ $(C-\bar{g}_i-\bar{g}_{i+1})$	$\left(q_{1,i-1}\times g_{i-1}+q_{2,i-1}\times(C-g_i-g_{i-1})\right)/(s\times L_i-q_{2,i-1})$ $\left(\left(\bar{q}_{1,i+1}\times\bar{g}_{i+1}+\bar{q}_{2,i+1}\times(C-\bar{g}_i-\bar{g}_{i+1})\right)/(s\times\bar{L}_i-\bar{q}_{2,i+1})\right)$	0
6	$C-g_{i-1}$ $(C-\bar{g}_{i+1})$	$g_{i-1}-g_i$ $(\bar{g}_{i+1}-\bar{g}_i)$	$\left(q_{2,i-1}\times(C-g_{i-1})+q_{1,i-1}\times(g_{i-1}-g_i)\right)/(s\times L_i-q_{1,i-1})$ $\left(\left(\bar{q}_{2,i+1}\times(C-\bar{g}_{i+1})+\bar{q}_{1,i+1}\times(\bar{g}_{i+1}-\bar{g}_i)\right)/(s\times\bar{L}_i-\bar{q}_{1,i+1})\right)$	0

where, $\gamma_{1,i}=\theta_i+C\times c_{1,i}-\left(\theta_{i-1}+t_{c,i-1}\right)$, $\bar{\gamma}_{1,i}=\theta_i+C\times c_{1,i}-\left(\theta_{i+1}+\bar{t}_{c,i}\right)$, $\gamma_{2,i}=\theta_i+C\times c_{2,i}-\left(\theta_{i-1}+g_{i-1}+t_{c,i}\right)$, $\bar{\gamma}_{2,i}=\theta_i+C\times c_{2,i}-\left(\theta_{i+1}+\bar{g}_{i+1}+\bar{t}_{c,i}\right)$

where λ denotes the bus arrival rate during the green phase. Then, the upper bound of a bus bandwidth for either direction can be computed as follows:

$$b_i^{\max}=arc\max_{b}\left\{\sum_{k=0}^{C_s}\frac{(\lambda_i b_i)^k\times e^{-\lambda_i b_i}}{k!}\geq p\right\} \tag{12}$$

$$\bar{b}_i^{\max}=arc\max_{\bar{b}}\left\{\sum_{k=0}^{C_s}\frac{\left(\bar{\lambda}_i\bar{b}_i\right)^k\times e^{-\bar{\lambda}\bar{b}_i}}{k!}\geq p\right\} \tag{13}$$

where Cs denotes the capacity of the bus stop and p is a parameter to indicate the reliability (e.g., 0.9). Eqs. (12) and (13) ensure the probability of spillover to be within a reasonable range. However, due to the inequality of interference constraints shown in (3) and (6), directly adding an upper bound $b_i^{max}(\bar{b}_i^{max})$ for $b_i(\bar{b}_i)$ may force the solution algorithm to simply reduce the value of $b_i(\bar{b}_i)$ without searching the feasible value for the control variables (i.e., offsets). As such, the resulting value of $b_i(\bar{b}_i)$ can be smaller than the maximum feasible bandwidth under the offset setting. Therefore, to ensure that the upper bound constraint for the green bandwidth can function effectively, one shall set the following constraints with a set of new binary variables, $s_i(\bar{s}_{i+1})$:

$$w_i-0.5\times b_i^{\max}\leq M\times s_i \tag{14}$$

$$w_i+0.5\times b_i^{\max}\geq g_i-M\times(1-s_i) \tag{15}$$

$$\bar{w}_{i+1}-0.5\times\bar{b}_i^{\max}\leq M\times\bar{s}_{i+1} \tag{16}$$

$$\bar{w}_{i+1}+0.5\times\bar{b}_i^{\max}\geq g_{i+1}-M\times(1-\bar{s}_{i+1}) \tag{17}$$

where, M is a large positive number that dominates all decision variables and parameters. Taking Eqs. (14)-(15) as an example, if s_i equals 1, it ensures that the time interval from the center of bus band to the end of a green phase is less than a half of the bandwidth's upper bound. Similarly, if s_i equals 0, it ensures that the time interval from the start of a green phase to the center of a bus band does not exceed a half of its upper bound.

4) Traffic Queue Clearance Constraints: Another important constraint is to account for the intersection traffic queue which relies highly on the total arriving traffic flows over a cycle. Given traffic volumes by movement, travel time for passenger cars between intersections, and signal timings, one can approximate the queue clearance time, τ_i, for a target intersection i based on an arrival traffic pattern as follows:

$$\tau_i=T_{3,i}+\frac{Q_{2,i}T_{1,i}+Q_{1,i}T_{2,i}-(s-Q_{1,i})T_{3,i}}{s-Q_{2,i}}=T_{3,i}+T_{4,i} \tag{18}$$

where $T_{1,i}$ and $T_{2,i}$ denote queue accumulating time before and after an incoming arrival flow change during a red phase at intersection i; $T_{3,i}$ and $T_{4,i}$ denote queue clearance time before and after an incoming arrival flow change during queue discharging at intersection*i, respectively*; $Q_{1,i}$ represent incoming arrival flow rates at intersection i during $T_{2,i}$ and $T_{3,i}$; $Q_{2,i}$ represent incoming arrival flow rates at intersection i during $T_{1,i}$ and $T_{4,i}$; and s denotes discharging flow rates.

Intermediate variables (i.e., $T_{1,i}$ to $T_{4,i}$) to calculate traffic queue clearance time for all arrival pattern type can be calculated, as shown in Table 2. With the time intervals specified shown in Table 2, one can compute the resulting queue clearance time, $\tau_i(\bar{\tau}_i)$ with the following constraints:

$$T_{1,i}+T_{2,i}=C-g_i\quad\text{for } i=1,\ldots,N \tag{19}$$

$$\bar{T}_{1,i}+\bar{T}_{2,i}=C-\bar{g}_i\quad\text{for } i=1,\ldots,N \tag{20}$$

$$\tau_i=T_{3,i}+T_{4,i}\quad\text{for } i=1,\ldots,N \tag{21}$$

$$\bar{\tau}_i=\bar{T}_{3,i}+\bar{T}_{4,i}\quad\text{for } i=1,\ldots,N \tag{22}$$

Eqs. (19)-(20) indicate the sum of $T_{1,i}$ and $T_{2,i}$, the queue accumulating period, is equal to the red interval. Eqs. (21)-(22) represent the sum of $T_{3,i}$ and $T_{4,i}$, indicating the queue discharging period or queue clearance time. Note that those time intervals in Eqs. (19)-(22) vary with the arrival traffic pattern types described in Fig. 4 and Table 2.

To facilitate model formulation of identifying an arrival traffic pattern type in Table 2, this study has further introduced

three sets of auxiliary binary variables:

$$x_{1,i} = 1, \quad if\ \theta_i + C \times c_{1,i} \le \theta_{i-1} + t_{c,i-1} \le \theta_i + g_i + C \times c_{1,i}; \quad 0, \quad otherwise \tag{23}$$

$$\bar{x}_{1,i} = 1, \quad if\ \theta_i + C \times \bar{c}_{1,i} \le \theta_{i+1} + \bar{t}_{c,i} \le \theta_i + \bar{g}_i + C \times \bar{c}_{1,i}; \quad 0, \quad otherwise \tag{24}$$

$$x_{2,i} = 1, \quad if\ \theta_i + C \times c_{2,i} \le \theta_{i-1} + g_{i-1} + t_{c,i-1} \le \theta_i + g_i + C \times c_{2,i}; \quad 0, \quad otherwise \tag{25}$$

$$\bar{x}_{2,i} = 1, \quad if\ \theta_i + C \times \bar{c}_{2,i} \le \theta_{i+1} + \bar{g}_{i+1} + \bar{t}_{c,i} \le \theta_i + \bar{g}_i + C \times \bar{c}_{2,i}; \quad 0, \quad otherwise \tag{26}$$

$$x_{3,i} = 1, \quad if\ x_{1,i} \ne x_{2,i}\ or \left(\begin{matrix} x_{1,i} = x_{2,i}\ and\ \theta_{i-1} + g_{i-1} + tc_{i-1} \\ = \theta_i + C \times c_{1,i} + x_{1,i} \times g_i + (1 - x_{1,i}) \times (C - g_i) \end{matrix} \right); \quad 0, \quad otherwise \tag{27}$$

$$\bar{x}_{3,i} = 1, \quad if\ \bar{x}_{1,i} \ne \bar{x}_{2,i}\ or \left(\begin{matrix} \bar{x}_{1,i} = \bar{x}_{2,i}\ and\ \theta_{i+1} + \bar{g}_{i+1} + \overline{tc}_i \\ = \theta_i + C \times \bar{c}_{1,i} + \bar{x}_{1,i} \times \bar{g}_i + (1 - \bar{x}_{1,i}) \times (C - \bar{g}_i) \end{matrix} \right); \quad 0, \quad otherwise \tag{28}$$

where $x_{1,i}$ ($\bar{x}_{1,i}$) is set to be 1 if the first possible leading through vehicle from the upstream outbound (inbound) intersection $i-1$ ($i+1$) encounters the green at the intersection i, otherwise 0; $x_{2,i}$ ($\bar{x}_{2,i}$) is set to 1 if the last possible lagging through vehicle from the outbound (inbound) upstream intersection $i-1$ ($i+1$) experiences the green phase at the intersection i, otherwise 0; and $x_{3,i}$ ($\bar{x}_{3,i}$) is set to 1 if through or turning flows from the upstream outbound (inbound) intersection $i-1$ ($i+1$) experience phase changes at the intersection i, otherwise 0. According to offsets, those three sets of introduced variables indicate which type of queue formation and discharging intersection i would experience. For example, when $x_{1,\mathrm{i}} = x_{2,\mathrm{i}} = 1$ and $x_{3,\mathrm{i}} = 0$, an arrival pattern of Type 1 causes queue formation and discharging at intersection i for outbound direction. The detailed formulation techniques adopted to ensure the linearity and corresponding time intervals during queue formation and discharging based on the types are introduced in Appendix-A

In brief, Model 1 (M-1) could be summarized as follows:

M-1 : $Max\ b + k_b \bar{b}$

s.t. Eqs. (2) – (10)

Eqs. (14) – (17)

Eqs. (19) – (28)

$b, \bar{b}, w_i, \bar{w}_i \ge 0$ for $i = 1, \ldots, N$

$n_i, \bar{n}_i, c_{1,i}, \bar{c}_{1,i}, c_{2,i}, \bar{c}_{2,i}$ are integer variables for $i = 1, \ldots, N x_{j,i}, \bar{x}_{j,i}, s_i, \bar{s}_i$ are binary variables, for $j = 1, 2, 3$, and $i = 1, \ldots, N. T_{j,i}, \bar{T}_{j,i} \ge 0\ for j = 1, \ldots, 4$ and $i = 1, \ldots, N \tau_i, \bar{\tau}_i, \gamma_{1,i}, \bar{\gamma}_{1,i}, \gamma_{2,i}, \bar{\gamma}_{2,i}, \theta_i \ge 0$ for $i = 1, \ldots, N$

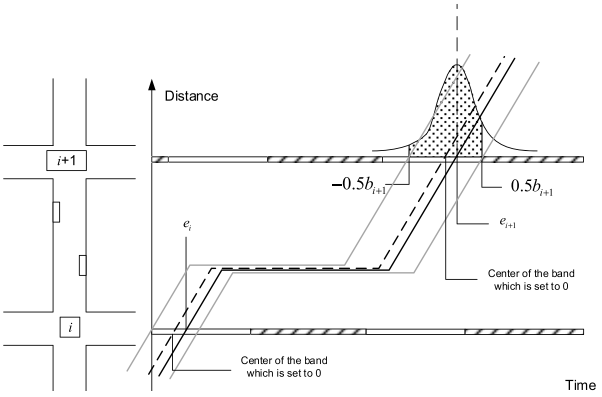

Fig. 6. Illustration of dwelling time variance between two adjacent intersections.

B. Model 2: An Enhanced Model Considering Bus Dwell Time Uncertainty

The enhanced model, proposed to account for dwell time uncertainty with variable bus bands along a segment, has the following revised objective function:

$$Max \sum\nolimits_i \varphi_i b_i^e + \sum\nolimits_i \bar{\varphi}_i \bar{b}_i^e \tag{29}$$

where $\varphi_i(\bar{\varphi}_i)$ is a weighting factor of intersection i for outbound (inbound) direction; and $b_i^e(\bar{b}_i^e)$ is the effective bandwidth for buses at intersection i. The weighting factor, $\varphi_i(\bar{\varphi}_i)$, can be specified with the expected number of outbound (inbound) buses per hour passing intersection i during the synchronized phase, m_i ($\bar{m}_i$), as follows:

$$\varphi_i = \frac{m_i}{\sum m_i + \sum \bar{m}_i} \quad \text{for } i = 1, \ldots, N \tag{30}$$

$$\bar{\varphi}_i = \frac{\bar{m}_i}{\sum m_i + \sum \bar{m}_i} \quad \text{for } i = 1, \ldots, N \tag{31}$$

The effective bandwidth, $b_i^e(\bar{b}_i^e)$, affecting the number of buses staying within the band at intersection i and its downstream intersection, can be defined as follows:

1) Scenario 1: No Bus Stop on a Link: If no bus stop is located between two consecutive intersections i and $i+1$, all buses in the progression band are expected to stay in the band, and the effective bandwidth shall be identical to the bandwidth for intersection $i(i+1)$, that is,

$$b_i^e = b_i \tag{32}$$

$$\bar{b}_{i+1}^e = \bar{b}_{i+1} \tag{33}$$

2) Scenario 2: Incorporating the Dwell Time Variance in the Formulations: If a bus stop is located between two consecutive intersections i and $i+1$, the effective bandwidth for intersection i can be calculated, based on the probability that a bus from the arriving band can stay within the departing band after leaving the bus stop. Fig. 6 shows an example of bus bands at two consecutive intersections, where the dashed line indicates the center of green bands and the solid line represents the trajectory of one bus moving in the outbound direction; e_i denotes the bus arrival time at intersection i, which is measured by its deviation from the center of the band.

Then, the expected arrival time of the bus at intersection $i+1$, e_{i+1}, shall equal e_i, because the travel time plus the expected dwell time is the horizontal difference between the centers of these two bands.

Assuming that all buses travel at the same speed within one cycle and their dwell times follow a normal distribution with a mean of μ_i and a standard deviation of σ_i, the arrival times to the downstream intersection shall follow a normal distribution, $\mathrm{N}(e_i, \sigma_i^2)$. Note that the time interval during which the bus passes both intersections are measured by their differences from the center of the bands. Then, the probability that the departing bus from a stop to stay in the departing band shall equal the probability that the actual arrival time to the downstream intersection is within the departing band of the bus stop, as shown in the shaded area in Fig. 6. Such a probability can be expressed as follows:

$$\begin{aligned} &P(-0.5b_{i+1} \le e_{i+1} \le 0.5b_{i+1}) \\ &= \Phi(\frac{0.5b_{i+1} - E\,(e_{i+1})}{\sigma_i}) - \Phi(\frac{-0.5b_{i+1} - E\,(e_{i+1})}{\sigma_i}) \\ &= \Phi(\frac{0.5b_{i+1} - e_{\mathrm{i}}}{\sigma_i}) - \Phi(\frac{-0.5b_{i+1} - e_{\mathrm{i}}}{\sigma_i}) \end{aligned} \tag{34}$$

where $E(e_{i+1})$ denotes the expectation of actual arrival time, which equals e_i. Note that the value of e_i shall lie between $-0.5b_i$ and 0.5 b_i. The effective bandwidth at intersection i can be obtained by integrating the probability with e_i as follows:

$$\begin{aligned} b_i^e &= \int_{-0.5b_i}^{0.5b_i} P\,(-0.5b_{i+1} \le e_{i+1} \le 0.5b_{i+1}) de_i \\ &= \int_{-0.5b_i}^{0.5b_i} \Phi(\frac{0.5b_{i+1} - e_i}{\sigma_i}) - \Phi(\frac{-0.5b_{i+1} - e_i}{\sigma_i}) de_i \end{aligned} \tag{35}$$

where b_i^e denotes the effective bandwidth at intersection i. By the same token, the inbound effective bandwidth can be expressed as follows:

$$\bar{b}_{i+1}^e = \int_{-0.5\bar{b}_{i+1}}^{0.5\bar{b}_{i+1}} \Phi(\frac{0.5\bar{b}_i - \bar{e}_{i+1}}{\bar{\sigma}_i}) - \Phi(\frac{-0.5\bar{b}_i - \bar{e}_{i+1}}{\bar{\sigma}_i}) d\bar{e}_{i+1} \tag{36}$$

In summary, for those links without a bus stop, the effective bandwidth can be directly obtained with (32)-(33). In contrast, for other links with a bus stop, one shall take into account the impact caused by bus dwell time uncertainty and apply (35)-(36) to estimate the effective bandwidth.

Conceivably, a larger effective bandwidth can guarantee a higher number of transit vehicles to receive the progression at two consecutive intersections. Hence, the total effective bandwidth for each pair of intersections along the arterial can serve as an indicator to evaluate the effectiveness of a signal plan. However, Eqs. (35) and (36) are highly non-linear in nature due to the adoption of integral and normal distributions. To improve the computing efficiency, the linearization steps introduced in Appendix-B have been taken to yield the optimal solution.

Also note that in Model 2, since the bandwidths are allowed to be varying at the bus stop, the interference constraints need to be revised as follows:

$$w_i - 0.5b_i \ge \tau_i \quad \text{for } i = 1, \ldots, N \tag{37}$$

$$w_i + 0.5b_i \le g_i \quad \text{for } i = 1, \ldots, N \tag{38}$$

$$w_i - 0.5\bar{b} \ge 0 \quad \text{for } i = 1, \ldots, N \tag{39}$$

$$\bar{w}_i + 0.5\bar{b} \ge \bar{g}_i - \bar{\tau}_i \quad \text{for } i = 1, \ldots, N \tag{40}$$

In brief, Model 2 (M-2), incorporating stochastic dwell times in computing bus progression bands, can be summarized as follows:

$$\begin{aligned} M-2\text{:}\ \ & Max \sum\nolimits_i \varphi_i b_i^e + \sum\nolimits_i \bar{\varphi}_i \bar{b}_i^e \\ & \text{s.t. Eqs}(37) - (40) \\ & \quad \text{Eqs.}(7) - (10) \\ & \quad \text{Eqs.}(14) - (17) \\ & \quad \text{Eqs.}(19) - (28) \\ & \quad \text{Eqs.}(30) - (33) \\ & \quad \text{Eqs.}(B1) - (B10) \\ & \quad b_i^e, \bar{b}_i^e, w_i, \bar{w}_i, H_{ik} \ge 0 \quad \text{for } i = 1, \ldots, N \\ & \quad n_i, \bar{n}_i, c_{1,i}, \bar{c}_{1,i}, c_{2,i}, \bar{c}_{2,i} \text{ are integer variables} \\ & \quad \text{for } i = 1, \ldots, N x_{j,i}, \bar{x}_{j,i}, s_i, \bar{s}_i \text{ are binary} \\ & \quad \text{variables, for } j = 1, 2, 3, \text{ and } i = 1, \ldots, N \\ & \quad T_{j,i}, \bar{T}_{j,i} \ge 0 \quad \text{for } j = 1, \ldots, 4, \text{ and } i = 1, \ldots, N \\ & \quad \tau_i, \bar{\tau}_i, \gamma_{1,i}, \bar{\gamma}_{1,i}, \gamma_{2,i}, \bar{\gamma}_{2,i}, \theta_i \ge 0 \text{ for} i = 1, \ldots, N \end{aligned}$$

IV. Numerical Analysis

The experimental analysis first evaluates the quality of bus progression produced by the proposed models in terms of the percentage of buses which can actually experience the progression along the target arterial. This study also assesses the operational performance with respect to bus travel times. The overall network performance is then included in the evaluation. The results are compared with the base progression plan, generated by MULTIBAND [21], the state-of-art model in the literature for signal progression. To be specific, signal progression plans for numerical analysis are produced from the following three models:

- Model 1 (M-1): A two-way progression model designed for buses, which is an extension of MAXBAND by adding the average bus dwell time, bus stop capacity, and queue clearance time constraints
- Model 2 (M-2): A two-way progression model designed for buses, which is an extension of M-1 with variable bands along an arterial to account for dwell time uncertainty
- MULTIBAND: a two-way progression model designed for passenger cars [21]

In this section, all mixed-integer-linear-programming problems are solved in CPLEX ILOG which is operated on a desktop with 8GB RAM and Intel i7 processor.

A. Experimental Design

To evaluate the potential of the proposed models for real-world applications, this study selects an arterial segment

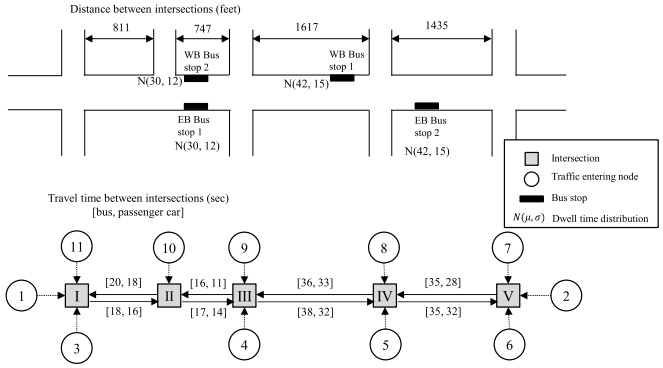

Demand Level	Input traffic volume (vph) at each input node [1 , 2 , 3 , 4 , 5 , 6 , 7 , 8 , 9 , 10 , 11]
1	[900, 900, 50, 100, 200, 50, 50, 200, 100, 50, 120]
2	[1200, 1200, 60, 120, 250, 60, 60, 250, 120, 60, 150]
3	[1800, 1800, 80, 150, 400, 80, 80, 400, 200, 80, 250]
4	[2100, 2100, 100, 200, 500, 100, 100, 500, 300, 100, 300]
5	[2300, 2300, 200, 200, 600, 200, 200, 600, 300, 200, 400]

Fig. 7. Simulation Settings.

on Dongzhimenwai Road in Beijing for case study. The simulation network consists of five intersections with two roadside bus stops in each direction. The key features such as geometry and traffic conditions used in the analysis are summarized in Fig. 7. Note that the bus dwell times at a bus stop in each direction are assumed to follow normal distributions with mean and standard deviation (seconds) as shown in Fig. 7 besides the bus stops. The five intersections have the common cycle length of 150 seconds. The outbound and inbound traffic flows share the same signal phases at intersections I to V with the timings 70, 120, 105, 55, and 108 seconds, respectively.

To test the performance under different dwell time variances, three dwell time standard deviations of zero (constant dwell time), 5 seconds, and 12/15 seconds are evaluated under the same average dwell times. To analyze the impacts of passenger car volume on bus progression, five volume scenarios have been applied in the case study (Fig. 7).

To evaluate the network performance under different optimization models, this study adopts VISSIM, microscopic multi-modal traffic flow simulation software, as a simulation platform. The transit routes along the arterial are added to the network with pre-specified entering headways, and the dwell times at each bus stop are assumed to follow normal distributions. The signal plan, produced from each model for comparison, has been simulated with all scenarios of different traffic volumes and different dwell time variances. The standard exercise of fifteen-minute warm-up period and one hour simulation times are adopted in the simulation experiments. To assess the quality of bus progression, an average of 12 buses per hour in each direction is set to be the bus demand, and all buses are simulated to pass the first intersection during the green phase in the designed band. For the network performance, a total of 60 buses per hour in each direction were scheduled to follow a uniform distribution to enter the network for simulation. Due to the stochastic nature of the employed microscopic traffic simulation program, each scenario has been simulated with ten simulation replications with different random seeds.

B. Model Evaluation I: Bus Progression

Table 3 summarizes the level of progression experienced by those buses under various simulated environments. Under the plan of MULTIBAND, more than 50 percent of buses encounter one or more stops at the intersections along the arterial, which may cause unstable travel times. For example, under zero dwell time deviation and low traffic volume condition, only 48% of buses pass the arterial without stop, but 5% of buses experience one stop, and 47% of buses experience two stops. The percentage of buses experiencing progression decreases with an increase in traffic demand or dwell time deviation. For example, under the scenario of medium traffic volume and high dwell time deviation (i.e., Demand 3 and dwell time deviations of 12/15 seconds), only 30% of buses under MULTIBAND proceed through the arterial without stops at intersections, where 35% of buses experience one stop; 20% of buses experience two stops; and 15 % of buses stop at three intersections.

In comparison, M-1 plan provides a better progression for buses under zero or five second dwell time deviations, and also under low or medium traffic volume (i.e., Demand-1 to Demand-3) where most buses (more than 90% of buses) pass the arterial without stops. Yet as passenger car flows increase to a high volume level (i.e., Demand 5 with the same dwell time deviation), 56 % (compared to 28% in MULTIBAND) of buses enjoy the full progression; 18% (29 % in MULTIBAND) of buses stop at one intersection; and other 26 % (34 % in MULTIBAND) of buses stop at two intersections. The results evidence the impacts of traffic congestion and the resulting passenger car queues on the bus running time between intersections and the progression quality. Under the scenarios of having the dwell time deviation of 5 (seconds), all buses under M-1 plan pass the arterial without stop at Demand-1, but 5% of buses start to experience one stop at Demand-2. As traffic demands increase, more buses are off from the progression band. For example, at Demand-4 only 56 % (39% in MULTIBAND) of buses enjoy the full progression, whereas 24% of buses stop at one intersection, and other 20 % of buses stop at two intersections. With a higher dwell time deviation of 12/15 (seconds), there are still some buses which can experience progression at all demand levels. For example, at Demand-4, 54% of buses can progress through all intersections without stop; 29% of buses stop at one intersection; other 15 % of buses stop at two intersections; and 2% of buses stop at three intersections. Notably, the percentage of buses that enjoy the progression, when experiencing even a small dwell variance, are generally less than those having constant dwell time.

Further evaluation results on the performance of M-2, designed to mitigate the impacts of dwell time variance on progression quality, confirm its effectiveness. For example, in the scenario with dwell time deviation of 5 (seconds) and Demand-4, M-2 allows only 2% of buses to experience two stops, whereas M-1 results in 20% of buses taking more than

TABLE III
NUMBER OF INTERSECTIONS WHERE A BUS STOPS RUNNING ALONG THE ARTERIAL WITH MULTIBAND, M-1 AND M-2

			MULTIBAND					M-1					M-2				
Dwell time deviation	Demand level		1	2	3	4	5	1	2	3	4	5	1	2	3	4	5
0 (s)	# of intersection stopped	0	48%	49%	48%	47%	28%	100%	100%	90%	61%	56%	-	-	-	-	-
		1	5%	6%	15%	3%	29%	0%	0%	7%	19%	18%	-	-	-	-	-
		2	47%	45%	33%	20%	34%	0%	0%	3%	20%	26%	-	-	-	-	-
		3	0%	0%	4%	30%	9%	0%	0%	0%	0%	0%	-	-	-	-	-
		4	0%	0%	0%	0%	0%	0%	0%	0%	0%	0%	-	-	-	-	-
5 (s)	# of intersection stopped	0	38%	39%	38%	37%	27%	100%	95%	90%	56%	56%	84%	84%	74%	72%	43%
		1	20%	20%	25%	25%	29%	0%	4%	8%	24%	23%	16%	16%	25%	26%	51%
		2	37%	35%	30%	30%	30%	0%	1%	2%	20%	21%	0%	0%	1%	2%	6%
		3	5%	6%	7%	8%	14%	0%	0%	0%	0%	0%	0%	0%	0%	0%	0%
		4	0%	0%	0%	0%	0%	0%	0%	0%	0%	0%	0%	0%	0%	0%	0%
12, 15 (s)	# of intersection stopped	0	35%	33%	30%	32%	22%	83%	70%	68%	54%	46%	83%	78%	76%	59%	41%
		1	32%	29%	35%	31%	32%	16%	26%	25%	29%	37%	17%	21%	24%	36%	49%
		2	25%	28%	20%	23%	31%	1%	4%	5%	15%	17%	0%	0%	0%	5%	9%
		3	8%	10%	15%	14%	15%	0%	0%	1%	2%	0%	0%	0%	0%	0%	0%
		4	0%	0%	0%	0%	0%	0%	0%	0%	0%	0%	0%	0%	0%	0%	0%

1 stop along the arterial. Under a higher dwell time deviation of 12/15 (seconds), M-2, as expected, outperforms the other two models in Demand-4, where M-1 has 54 % of buses enjoying the full progression; 29% of buses stop at one intersection; another 15 % of buses stop at two intersections; and 2% of buses stop at three intersections. In contrast, M-2 allows 95% of buses to enjoy the progression with zero or one stop, and only 5% of the total buses experience more than one stop along the target arterial. Hence, the incorporation of dwell time uncertainty has clearly shown its contribution to achieving better bus progression by reducing the number of buses that experience frequent stops along an arterial.

In brief, the above numerical analyses with the MOE of bus progression effectiveness clearly show that:

- The state-of-the-art model, MULTIBAND, designed mainly for passenger car flows, cannot offer the same quality of progression for bus flows.
- M-1 model which incorporates the impacts of intersection queue from passenger car flows on car indeed offers progression bands for most buses under most scenarios with low dwell variances.
- The bus progression quality, especially when experiencing high dwell time variance, can be further improved by M-2 model which includes dwell time uncertainly and intersection traffic queue impacts on the offset computation.

Fig. 8 shows the average bus travel time under three candidate signal progression plans with high dwell time deviation, where M-2 clearly outperforms the other two models. Again, the conventional model for progression of passenger cars cannot offer the same benefits to bus flows as with our proposed models.

C. Model Evaluation II: Network Performance

To evaluate the network performance under the bus progression plans, the following measures of effectiveness are adopted for model assessment: average passenger car delay, average bus vehicle delay, and average person delay. The average person delay is computed with the following equation:

$$d_p = \frac{\rho_c \cdot q_c \cdot d_c + \rho_b \cdot q_b \cdot d_b}{\rho_c \cdot q_c + \rho_b \cdot q_b} \tag{41}$$

where, d_p, d_c and d_b denote the average person delay, average passenger car delay, average bus delay, respectively; ρ_c and ρ_b represent the loading factor of passenger cars and buses and set to be 1.2 and 30, respectively; q_c and q_b are the flow rates of passenger cars and buses, respectively. The scenario of Demend-3 and dwell time deviation of 12/15 seconds is applied in the experimental analyses.

Analyses with the above MOEs have yielded the following findings:

- Overall, M-1 and M-2 can offer operational benefits to transit vehicles by reducing average bus delay by 14.00% and 17.03%, respectively, compared to the results with MULTIBAND (Fig. 9). Due to the trade-off nature, M-1 and M-2 cause an increase in the average passenger car delay by 2.02% and 14.75%, compared to the results with MULTIBAND (Fig. 9).

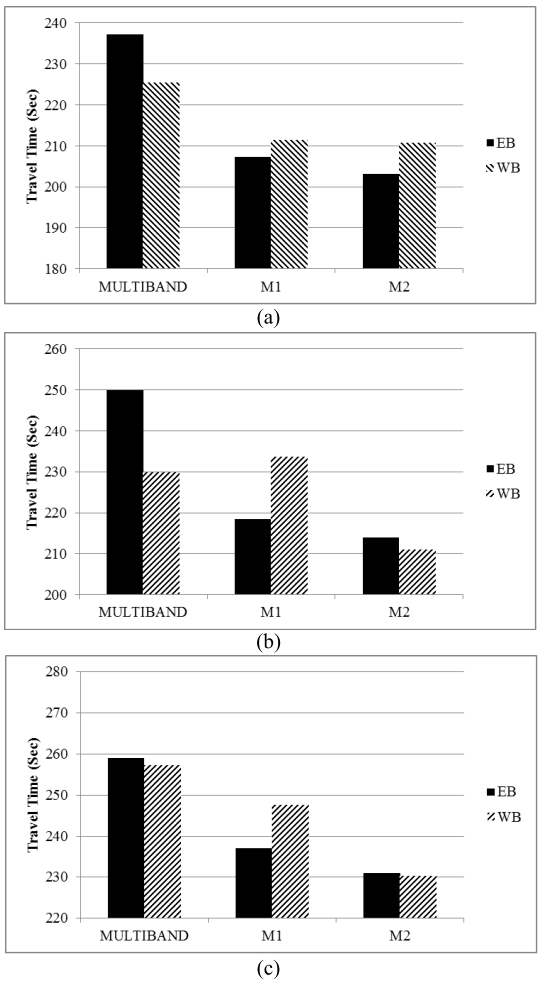

Fig. 8. Average bus travel times (a) demand 1, (b) demand 3, and (c) demand 5.

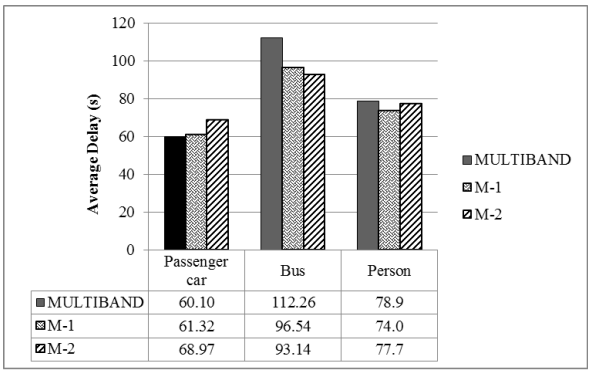

Fig. 9. Average delays for passenger car, bus, and person.

- M-1 and M-2 have reduced the average person delay by 6.20% and 1.55%, respectively, compared to the results with MULTIBAND (Fig. 9).
- With an increase in bus loading factor, M-1 and M-2 contribute more to the reduction in average person delay. For example, when loading factors of passenger car and bus are 1.2 and 40 respectively, M-1 and M-2 decrease the average person delay by 7.3% and 3.8% respectively, compared to MULTIBAND (Fig. 10).

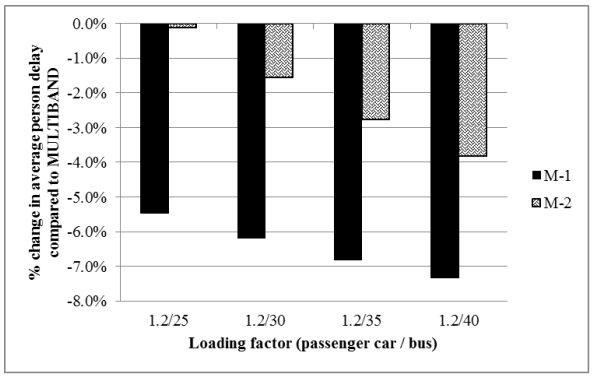

Fig. 10. Impacts of loading factors on average person delay.

- Signal plans under M-1 and M-2 can decrease the percentage of buses to stop along the arterial, compared to the results with MULTIBAND. Those buses under the plans by M-1 and M-2 show an average intersection stop of 1.64 and 1.69, respectively, less than 2.07 stops under MULTIBAND. The bus progression quality under M-2 plan also shows a better stability than M-1 plan, as evidenced in the resulting standard deviation of intersection stops (i.e. 0.70 for M-2 vs. 0.79 for M-1), showing the advantage of considering bus dwell time uncertainty in the proposed model.

V. Conclusions

Existing TSP control strategies may not be applicable to arterials with heavy bus volume due to excessive activations and negative impacts on the network. Under such circumstances, a passive control strategy, directly considering the bus volume in design of signal offsets, can be a viable option to facilitate bus flows and to increase bus ridership.

This paper has first presented a base signal progression model to optimize the offsets for an urban arterial that needs to accommodate transit flows with high passenger demand. To ensure that the bus progression would not be interrupted by the traffic queues at intersections, the traffic queues calculated with offsets need to be cleared ahead of the progression band. The enhanced model further accounts for the dwell time variation which varies with the distribution of transit passenger demands.

The results of extensive numerical investigations confirmed that the proposed models can indeed provide a progression to buses under different traffic conditions and different levels of dwell time certainty. The results also demonstrated that the proposed models can improve bus operational performance in terms of the number of stopped intersections, bus travel times, and average delay with acceptable impacts on passenger cars compared to the results with MULTIBAND. It is also shown that the enhanced model, considering the stochastic nature of bus dwell time, further improves the travel conditions for passengers on buses.

The proposed models have potential to be extended to a network with multiple bus routes. In real urban networks, multiple bus routes may share a segment on an arterial

while some may leave the arterial with turnings at different intersections. Limited by the article length, the formulation and experiments in this paper focus only on through movement along an arterial. Further studies focusing on bus progression design applied to networks should account for issues discussed in this paper and concepts for multi-path progression [23] and network progression [32]. Other further extensions along this line will be focused on advancing the proposed model to account for the location of bus stops and speed differences between passenger cars and transit vehicles under various traffic conditions. The cooperation of the offline signal plan and real-time control to further improve bus operation is also a promising research direction.

APPENDIX-A

One can convert an equal constraint for a certain condition (A1) into (A2) and (A3) as follows:

$$f1\left(x\right) = f2\left(x\right) \tag{A1}$$

when $y_i = 1$ and $y_j = 1$

$$f1\left(x\right) \geq f2\left(x\right) - M\left(2 - y_i - y_j\right) \tag{A2}$$

$$f1\left(x\right) \leq f2\left(x\right) + M\left(2 - y_i - y_j\right) \tag{A3}$$

Also, a constraint of minimum between two values, (A4), can be converted into (A5) - (A11) as follows:

$$f3\left(x\right) = \min\left[f1\left(x\right), f2\left(x\right)\right] \tag{A4}$$

$$f1\left(x\right) - f2\left(x\right) \leq Mz_1 \tag{A5}$$

$$f1\left(x\right) - f2\left(x\right) \leq Mz_2 \tag{A6}$$

$$z_1 + z_2 = 1 \tag{A7}$$

$$f3\left(x\right) \geq f2\left(x\right) + M\left(1 - z_1\right) \tag{A8}$$

$$f3\left(x\right) \leq f2\left(x\right) + M\left(1 - z_1\right) \tag{A9}$$

$$f3\left(x\right) \geq f1\left(x\right) + M\left(1 - z_2\right) \tag{A10}$$

$$f3\left(x\right) \leq f1\left(x\right) + M\left(1 - z_2\right) \tag{A11}$$

APPENDIX-B

A. Step 1: Discretizing the Arriving Band

First, the arriving band at the upstream intersection is divided into several small intervals. For each small interval in the band, the effective bandwidth is calculated based on its associated interval in the distribution. To define the boundaries of those intervals, one can introduce the following linear constraints for the outbound bands:

$$u_{ik}\frac{0.5b_{i+1} - \left(-0.5b_i + k \times \alpha\right)}{\sigma_i} - MI_{ik} \tag{B1}$$

$$u'_{ik} = \frac{-0.5b_{i+1} - \left(-0.5b_i + k \times \alpha\right)}{\sigma_i} - MI_{ik} \tag{B2}$$

where $u_{ik}(u'_{ik})$ represents the variate of the standard normal distribution in Eq. (36) ((37)) for interval k, whose length is α of the cycle length; I_{ik} is a binary variable, indicating whether or not interval k is within the green band. These two equations show the expression of those two terms at the right-hand side of Eq. (36) for buses departing from the upstream band at different times.

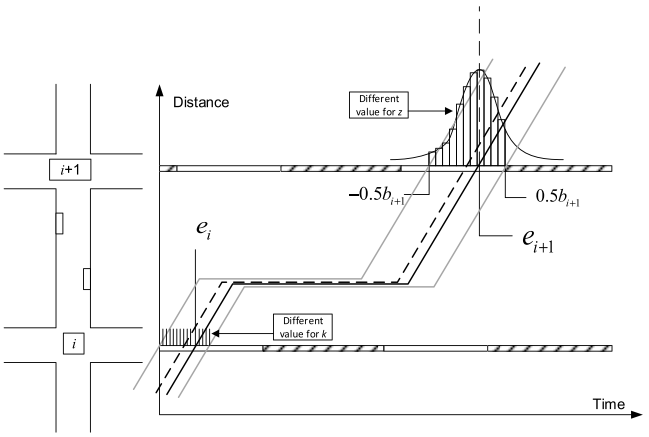

Fig. 11. Linearization method of the enhanced model.

By applying (B1)-(B2), buses passing the upstream intersection during interval k are considered to pass at the beginning of that period, as shown in Fig. 11. Since only the buses from the upstream band are considered, (B1)-(B2) should be invalid when the considered time point is out of the upstream band. This is accomplished by introducing the following binary variables, I_{ik}, which indicates whether the corresponding value of k is within the reasonable range.

$$I_{ik} < \frac{k \times \alpha - b_i}{M} + 1 \tag{B3}$$

$$I_{ik} \geq \frac{k \times \alpha - b_i}{M} \tag{B4}$$

Through (B3) and (B4), when the total length of k intervals is greater than the bandwidth, u_{ik} and u'_{ik} are set to be small enough not to contribute to the calculation of effective bandwidth and then, the lower and upper limit of integration in Eq. (35) can be determined.

B. Step 2: Estimating the Probability of Vehicles Staying in the Departing Band

Given the results of step 1, the value of $u_{ik}(u'_{ik})$ is used to determine the probability with Eq. (34). To estimate the probability that a vehicle from an interval remains in the band when reaching its downstream intersection, one can formulate this process as shown below:

$$y^z_{ik} < \frac{u_{ik} - \left(-\beta + z \times \gamma\right)}{M} + 1 \tag{B5}$$

$$y^z_{ik} \geq \frac{u_{ik} - \left(-\beta + z \times \gamma\right)}{M} \tag{B6}$$

$$y'^z_{ik} < \frac{u'_{ik} - \left(-\beta + z \times \gamma\right)}{M} + 1 \tag{B7}$$

$$y'^z_{ik} \geq \frac{u'_{ik} - \left(-\beta + z \times \gamma\right)}{M} \tag{B8}$$

$$H_{ik} = \sum_{z=1}^{Z} n_z\left(y^z_{ik} - y'^z_{ik}\right) \tag{B9}$$

where,

- n_z is the cumulative density of the z-th interval of the standard normal distribution, $n_z = \Phi\left(-\beta + \gamma \times (z+1)\right) - \Phi\left(-\beta + \gamma \times z\right)$.

- $y_{ik}^{z}(y'z_{ik})$ is a binary variable, indicating whether or not the resulting variate is greater than a certain value, which will determine the interval where $u_{ik}(u'_{ik})$ exists.
- γ is the length of intervals, shown as the width of rectangular at the top right part of Fig. 11.
- H_{ik} is the approximate probability that a bus from interval k will stay in the band when passing the downstream intersection, which is expressed as Eq. (35).

By defining the value for series of binary variables, $y_{ik}^{z}(y_{ik}'^{z})$, (36)–(37) and (B1)-(B2) will determine which rectangular under the cumulative density function should be included in calculation of the probability. Equation (B9) sums up the corresponding area of the rectangles to obtain the total probability (approximation of the exact probability) which is expressed as the rectangular area in Fig. 11.

C. Step 3: Finding the Effective Bandwidth

By multiplying the length of each small interval and its corresponding probability, one can obtain the equivalent effective portion of the interval, and then use Eq. (B10) to sum up the resulting effective portion to obtain the total effective bandwidth as follows:

$$b_i^e = \sum_{k=1}^{K} \alpha H_{ik} \tag{B10}$$

Given the linearized effective bandwidths, the size of k, which should be sufficiently large to keep the approximation reasonable, is set to equal 20. The range of z, denoting the number of intervals within the arriving band, and the value of β andγ, shall be so determined to ensure that $\Phi(-\beta+\gamma)$ is sufficiently small and $\Phi(-\beta+Z\times\gamma)$ is close to 1. For example, this study assumes $\beta = -2.8$, $\gamma = 0.4$, and $Z = 13$, then the segment $(-2.4, 2.4)$ on x axis is divided into 12 intervals, each having a value for n_z, the cumulative density. The constraints for inbound directions are specified in the similar structure. The effective bandwidths for inbound direction can be calculated with the same logic.

REFERENCES

[1] T. Urbanik, II, "Priority treatment of buses at traffic signals," in *Proc. Transp. Eng.*, 1977, pp. 31–33.

[2] J. S. Ludwick, Jr, "Simulation of an unconditional preemption bus priority system," Mitre Corp., McLean, VA, USA, Rep. MTP-400, 1974.

[3] F. Dion and H. Rakha, "Integrating transit signal priority within adaptive traffic signal control systems," presented at the 84th Annu. Meeting Transp. Res. Board, Washington, DC, USA, 2005.

[4] H. R. Smith, B. Hemily, and M. Ivanovic, *Transit Signal Priority (TSP): A Planning and Implementation Handbook*. Washington, DC, USA: ITS Amer., 2005.

[5] K. N. Balke, C. L. Dudek, and I. T. Urbanik, "Development and evaluation of an intelligent bus priority concept," presented at the 79th Annu. Meeting Transp. Res. Board, Washington, DC, USA, 2000.

[6] M. Janos and P. Furth, "Bus priority with highly interruptible traffic signal control: Simulation of San Juan's Avenida ponce de leon," *Transp. Res. Rec., J. Transp. Res. Board*, vol. 1811, pp. 157–165, Jan. 2002.

[7] T. Satiennam, T. Muroi, A. Fukuda, and S. Jansuwan, "An enhanced public transportation priority system for two-lane arterials with nearside bus stops," in *Proc. Eastern Asia Soc. Transp. Stud.*, vol. 5. 2005, pp. 1309–1321.

[8] Y. Lin, X. Yang, G.-L. Chang, and N. Zou, "Transit priority strategies for multiple routes under headway-based operations," *Transp. Res. Rec., J. Transp. Res. Board*, vol. 2356, pp. 34–43, Nov. 2013.

[9] M. Li, Y. Yin, W.-B. Zhang, K. Zhou, and H. Nakamura, "Modeling and implementation of adaptive transit signal priority on actuated control systems," *Comput.-Aided Civil Infrastructure Eng.*, vol. 26, no. 4, pp. 270–284, 2011.

[10] G.-L. Chang, M. Vasudevan, and C.-C. Su, "Modelling and evaluation of adaptive bus-preemption control with and without automatic vehicle location systems," *Transp. Res. A, Policy Pract.*, vol. 30, no. 4, pp. 251–268, 1996.

[11] E. Christofa, K. Ampountolas, and A. Skabardonis, "Arterial traffic signal optimization: A person-based approach," *Transp. Res. C, Emerg. Technol.*, vol. 66, pp. 27–47, May 2016.

[12] G. T. Bowen, R. D. Bretherton, J. R. Landles, and D. J. Cook, "Active bus priority in SCOOT," in *Proc. 7th Int. Conf. Road Traffic Monitoring Control*, 1994, pp. 73–76.

[13] P. Mirchandani, A. Knyazyan, L. Head, and W. Wu, "An approach towards the integration of bus priority, traffic adaptive signal control, and bus information/scheduling systems," in *Computer-Aided Scheduling of Public Transport*. Berlin, Germany: Springer, 2001, pp. 319–334.

[14] M. Keyvan-Ekbatani, A. Kouvelas, I. Papamichail, and M. Papageorgiou, "Exploiting the fundamental diagram of urban networks for feedback-based gating," *Transp. Res. B, Methodol.*, vol. 46, no. 10, pp. 1393–1403, 2012.

[15] K. Aboudolas, and N. Geroliminis, "Perimeter and boundary flow control in multi-reservoir heterogeneous networks," *Transp. Res. B, Methodol.*, vol. 55, pp. 265–281, Sep. 2013.

[16] K. Ampountolas, N. Zheng, and N. Geroliminis, "Macroscopic modelling and robust control of bi-modal multi-region urban road networks," *Transp. Res. B, Methodol.*, vol. 104, pp. 616–637, Oct. 2017.

[17] M. Keyvan-Ekbatani, M. Papageorgiou, and I. Papamichail, "Urban congestion gating control based on reduced operational network fundamental diagrams," *Transp. Res. C, Emerg. Technol.*, vol. 33, pp. 74–87, Aug. 2013.

[18] J. T. Morgan and J. D. C. Little, "Synchronizing traffic signals for maximal bandwidth," *Oper. Res.*, vol. 12, no. 6, pp. 896–912, 1964.

[19] J. D. C. Little, "The synchronization of traffic signals by mixed-integer linear programming," *Oper. Res.*, vol. 14, no. 4, pp. 568–594, 1966.

[20] J. Little, M. D. Kelson, and N. H. Gartner, "MAXBAND: A program for setting signals on arteries and triangular networks," *Transp. Res. Rec.*, vol. 795, pp. 40–46, Jun. 1981.

[21] N. H. Gartner, S. F. Assman, F. Lasaga, and D. L. Hou, "A multi-band approach to arterial traffic signal optimization," *Transp. Res. B, Methodol.*, vol. 25, no. 1, pp. 55–74, 1991.

[22] N. A. Chaudhary, V. G. Kovvali, C.-L. Chu, J. Kim, and S. M. Alam, "Software for timing signalized arterials," Texas Transp. Inst., Texas A&M Univ. Syst., College Station, TX, USA, Tech. Rep. FHWA/TX-03/4020-1, 2002.

[23] X. Yang, Y. Cheng, and G.-L. Chang, "A multi-path progression model for synchronization of arterial traffic signals," *Transp. Res. C, Emerg. Technol.*, vol. 53, pp. 93–111, Apr. 2015.

[24] N. Papola, "Bandwidth maximization: Split and unsplit solutions," *Transp. Res. B, Methodol.*, vol. 26, no. 5, pp. 341–356, 1992.

[25] C. J. Messer, R. H. Whitson, C. L. Dudek, and E. J. Romano, "A variable-sequence multiphase progression optimization program," *Highway Res. Rec.*, no. 445, pp. 24–33, 1973.

[26] H.-S. Tsay and L.-T. Lin, "A new algorithm for solving the maximum progression bandwidth," *Transp. Res. Rec.*, vol. 1194, no. 1194, pp. 15–30, 1988.

[27] L.-T. Lin, L.-W. Tung, and H.-C. Ku, "Synchronized signal control model for maximizing progression along an arterial," *J. Transp. Eng.*, vol. 136, no. 8, pp. 727–735, 2010.

[28] J.-Q. Li, "Bandwidth synchronization under progression time uncertainty," *IEEE Trans. Intell. Transp. Syst.*, vol. 15, no. 2, pp. 749–759, Apr. 2014.

[29] X. Yang, G. L. Chang, and S. Rahwanji, "Development of a signal optimization model for diverging diamond interchange," *J. Transp. Eng.*, vol. 140, no. 5, p. 04014010, 2014.

[30] E. C. Chang, S. L. Cohen, C. Liu, N. A. Chaudhary, and C. Messer, "MAXBAND-86: Program for optimizing left-turn phase sequence in multiarterial closed networks," *Transp. Res. Rec.*, vol. 906, no. 1181, pp. 61–67, 1988.

[31] N. A. Chaudhary and C. J. Messer, "Passer IV: A program for optimizing signal timing in grid networks (with discussion and closure)," *Transp. Res. Rec. Board*, vol. 1421, no. 1421, pp. 82–93, 1993.

[32] N. H. Gartner and C. Stamatiadis, "Arterial-based control of traffic flow in urban grid networks," *Math. Comput. Model.*, vol. 35, nos. 5–6, pp. 657–671, 2002.

[33] N. H. Gartner and C. Stamatiadis, "Progression optimization featuring arterial-and route-based priority signal networks," *J. Intell. Transp. Syst.*, vol. 8, no. 2, pp. 77–86, 2004.
[34] C. Zhang, Y. Xie, N. H. Gartner, C. Stamatiadis, and T. Arsava, "AM-band: An asymmetrical multi-band model for arterial traffic signal coordination," *Transp. Res. C, Emerg. Technol.*, vol. 58, pp. 515–531, Sep. 2015.
[35] W. Ma and X. A. Yang, "A passive transit signal priority approach for bus rapid transit system," in *Proc. IEEE ITS Conf.*, Sep. 2017, pp. 413–418.
[36] Y. Lin, X. Yang, N. Zou, and L. Jia, "A new passive transit signal priority control at urban arterials," (in Chinese), *J. Northeastern Univ., Natural Sci.*, vol. 34, no. 9, pp. 1227–1231, 2013.
[37] G. Dai, H. Wang, and W. Wang, "A bandwidth approach to arterial signal optimisation with bus priority," *Transportmetrica A, Transp. Sci.*, vol. 11, no. 7, pp. 579–602, 2015.
[38] G. Dai, H. Wang, and W. Wang, "Signal optimization and coordination for bus progression based on MAXBAND," *KSCE J. Civil Eng.*, vol. 20, no. 2, pp. 890–898, 2016.
[39] Y. Cheng, X. Yang, and G. Chang, "A bus-based progression system for arterials with heavy transit flows," in *Proc. 94th Annu. Meeting Compendium Papers*, 2015, p. 17.

Hyeonmi Kim received the B.S. and M.S degrees from Korea Aerospace University, South Korea, in 2005 and 2008, respectively. From 2007 to 2011, she was a Research Specialist with the Center for ITS Research, Korea Transport Institute, South Korea.

She is currently pursuing the Ph.D. degree with the Department of Civil and Environmental Engineering, University of Maryland, College Park, MD, USA. Her research interests include traffic control and operations, traffic safety, intelligent transportation system, and sustainable transportation.

Yao Cheng received the B.S. degree in transportation engineering from Tongji University, Shanghai, China, in 2012 and the M.S degree in civil and environmental engineering from University of Maryland, College Park, Maryland, in 2014.

He is currently pursuing the Ph.D. degree in civil and environmental engineering with University of Maryland, College Park, and is currently a Research Assistant with the Department of Civil and Environmental Engineering. His research interests include traffic operation and signal design.

Gang-Len Chang (M'13) received the B.Eng. degree from National Cheng Kung University, Tainan, Taiwan, in 1975; the M.S. degree from National Chiao Tung University, Hsinchu, Taiwan, in 1979; and the Ph.D. degree in transportation engineering from The University of Texas at Austin, TX, USA, in 1985.

He is currently a Professor with the Department of Civil and Environmental Engineering, University of Maryland, College Park, MD, USA. His current research interests include network traffic control, freeway traffic management and operations, real-time traffic simulation, and dynamic control of urban systems.

He is a member of the American Society of Engineers. He has served as the Chief Editor for ASCE *Journal of Urban Planning and Development* over the past 13 years.